Journal of Mines, Metals and Fuels, *71(12C) : 462-468; 2023. DOI: 10.18311/jmmf/2023/47306*

Print ISSN : 0022-2755

Journal of Mines, Metals and Fuels

Contents available at: *www.informaticsjournals.com/index.php/jmmf*

Radiation Effect on Heat and Mass Transfer of Casson Fluid owing to a Stretching Cylinder – A Numerical Approach

S. Sushma[1*], M. Uma[1], G. Neeraja[1], P. A. Dinesh[1] and G. K. Kalavathi[2]

[1]Department of Mathematics, M. S. Ramaiah Institute of Technology, Bengaluru – 560054, Karnataka, India; sush.msrit@gmail.com, umashivaram@gmail.com, n55raja@yahoo.co.in, dineshdpa@msrit.edu

[2]Department of Mathematics, Malnad College of Engineering, Hassan – 573202, Karnataka, India; gkk@mcehassan.ac.in

Abstract

A numerical study has been done to recognize the effects of non-Newtonian fluid outside a stretching absorbent cylinder with respect to radiation and suction or blowing. To model non-Newtonian fluid flow behavior Casson fluid is deliberated. To solve the leading differential equations similarity transformation is applied and finally the resultant equations are resolved mathematically with the assistance of shooting method. This work is contributed to know the effects of some of the factors such as Casson, radiation, suction/injection, Prandtl and Reynolds numbers for velocity, temperature and concentration profiles. The study is extended to know the effects of skin friction coefficient and temperature gradient and concentration gradient at the surface.

Keywords: *Casson Fluid, Radiation, Stretching Permeable Cylinder, Suction/Injection*

1.0 Introduction

Owing to the industrial applications, in the recent year's heat and mass transfer features of non-Newtonian fluids has gained significance. In order to model non-Newtonian fluid flow over a channel with definite yield value Casson fluid is considered. When it comes to the laminar boundary layers with stretching surfaces, has many engineering applications for instance in the manufacture and extraction of polymer and rubber sheets, glass fiber and paper making etc. In these applications many a times in order to get good quality product, the degree of cooling in stretching plays an important role[1]. Authors[2-4] contributed their study towards balanced flow of fluid outside stretching hollow cylinder. Ashorynejad *et al.*[5] has done a numerical study to analyze the flow of Nano fluid and its heat transfer in a stretching cylinder using similarity transformation with the existence of magnetic field and showed significant results on Reynolds number and magnetic factor. Similar studies on heat transfer in a stretching cylinder in company of magnetic field is analyzed in researches[6-8]. Abbas *et al.*[9,10] dedicated their work towards the heat transfer of hybrid Nano fluid over a stretching cylinder in the presence of inclined magnetic field using a numerical technique. Kumar *et al.*[11] conducted a numerical study to know the heat and mass transfer of a Nano fluid to achieve corrosion in the internal combustion engines by considering stretching cylinder.

Furthermore, the thermal radiation has a vital part in heat transmission and has many industrial and engineering applications such as extrusion process,

**Author for correspondence*

freezing of nuclear reactor, electronic equipment refrigerating etc. In view of these applications Islam *et al.*[12] analyzed analytically the flow of Nano fluid with the effects of radiation, joule heating and heat source over a stretching cylinder. Uma *et al.*[13,14] has done an analytical work to analyze the effects of radiation for a Couette flow of dusty viscoelastic fluid through a curly channel with and without thermal diffusion and diffusion thermo effects. Maleki *et al.*[15] has done a numerical work to know the influence of heat transmission characteristics of Nano fluid over porous plate by considering slip boundary conditions in the presence of radiation. Alnaqi *et al.*[16] calculated numerically heat transmission rate for a nano fluid with the occurrence of magnetic field and radiation in diagonal square cavity. Peiravi *et al.*[17] has made an attempt to know the effects of hybrid conduction or hybrid heat transfer since it improves the heat transfer mechanism in turn the thermal radiation through a rectangular cylinder by varying Reynolds number, radiation coefficients and emission coefficients. Makinde and Ogulu[18] analyzed numerically the effects of thermal radiation and heat and mass transmission behavior for an incompressible, laminar, steady flow operated in single direction in presence of diffused slanting magnetic field. The authors[19,20] contributed their study towards the analysis of heat and mass transfer for a steady and unsteady instances of a Nano fluid in presence of thermal radiation.

Since Casson fluid characterizes a non-Newtonian fluid, it is significant to study various properties related to the fluid flow. In view of some of industrial and bioengineering applications like metallurgy, food processing, drilling operations, in production of lubricants, paints, china clay and pharmaceutical products etc. Khan[21] has conducted a numerical comparative work to know the impact of Casson fluid with homogeneous and heterogeneous reactions. Heat and mass transmission of Casson fluid flow above a verticle surface with convective boundary conditions by considering triple diffusion which is solved numerically are discussed by Sushma *et al.*[22]. Some of the authors[23-26] dedicated their work towards Casson fluid flow for exponential stretching sheet. Mahdy[27] has done a numerical work in order to observe the heat transmission and flow nature of Casson fluid for stretching permeable cylinder by incorporating the effects of soret and Dufour.

The uniqueness of the present analysis is to review the effects of radiation and suction for steady two dimensional flow of Casson fluid in the process of heat and mass transfer due to stretching cylinder. It is detected from the earlier literature that many studies are directed for Casson fluid with or without thermal radiation for a stretching sheet. We have made an effort to study the flow performance of Casson fluid by stretching cylinder in company of suction/injection and radiation with a numerical approach.

2.0 Mathematical Formulation

Let us consider two-dimensional steady laminar non-Newtonian Casson fluid flow caused by a stretching tube of radius $'a'$ in the direction of axial axis when fluid is at rest, as shown in Figure 1, where axis of the tube is shown towards the $'z'$-axis and $'r'$-axis is towards radial direction. Assuming surface of the tube is constant $'T_w'$, the ambient fluid temperature is $'T_\infty'$, and $T_w > T_\infty$, assuming the tube is small viscous dissipation is ignored. The governing rheological state equations for the model is fluid[27] is

$$\tau_{ij} = \begin{cases} 2\left(\mu_B + \dfrac{P_y}{\sqrt{2\pi}}\right)e_j & \pi > \pi_c \\ 2\left(\mu_B + \dfrac{P_y}{\sqrt{2\pi_c}}\right)e_j & \pi < \pi_c \end{cases} \tag{1}$$

where, $\tau_{ij} = e_j\, e_j$, π indicates the product of constituents of deformation rate tensor with itself, π_c is a critical value of those product depending on non-Newtonian model. The fluid behaves like a solid if shear stress is smaller than yield stress whereas fluid behaves like moving if shear stress is bigger than yield stress. Under the assumptions of Bousinesq estimate for the body force the governing boundary layer equations is given as follows[27]: -

$$\frac{\partial(w)}{\partial z} + \frac{\partial(u)}{\partial r} = 0, \tag{2}$$

$$w\frac{\partial w}{\partial z} + u\frac{\partial w}{\partial r} = \nu\left(1 + \frac{1}{\beta}\right)\left(\frac{\partial^2 w}{\partial r^2} + \frac{1}{r}\frac{\partial w}{\partial r}\right), \tag{3}$$

$$w\frac{\partial T}{\partial z}+u\frac{\partial T}{\partial r}=K\left(\frac{\partial^2 T}{\partial r^2}+\frac{1}{r}\frac{\partial T}{\partial r}\right)+Q_0 \tag{4}$$

$$w\frac{\partial C}{\partial z}+u\frac{\partial C}{\partial r}=D\left(\frac{\partial^2 C}{\partial r^2}+\frac{1}{r}\frac{\partial C}{\partial r}\right) \tag{5}$$

Corresponding boundary settings of the model are [27]

$$u=U=-b\ \gamma,\ w=w_w=2b\ ,\ T=T_w,\ C=C_w,$$

when, $r=a$ (6)

$$w\to 0,\ T\to T_\infty,\ C\to C_\infty \text{ when } r\to\infty$$

In the above expression b is treated as positive constant. Also we have treated γ as constant taking into mass suction and mass injection when $\gamma>0$ and $\gamma<0$. Some of the non-dimensional parameters which are used in order to get a similarity solution

$$\eta=\frac{r^2}{a^2},\ w=2b\,f'(\eta)z,\ u=-\frac{b}{\sqrt{\eta}}f(\eta),$$

$$\theta(\eta)=\frac{T-T_\infty}{T_w-T_\infty},\ \phi(\eta)=\frac{C-C_\infty}{C_w-C_\infty} \tag{7}$$

Applying Equation (7) to Equations. (2) -(5), we get

$$\frac{1+\beta}{\beta}\left(\eta f'''+f''\right)+\mathbb{R}\left(ff''-f'^2\right)=0 \tag{8}$$

$$\theta''+\theta'+\mathbb{P}\ \mathbb{R}\ \theta'+Q=0 \tag{9}$$

$$\phi''+\phi'+\mathbb{S}\ \mathbb{R}\ \phi'=0 \tag{10}$$

Here primes denotes differentiation with respect to

$$\eta,\ \mathbb{P}=\frac{\nu}{\alpha},\ \mathbb{R}=\frac{b\,a^2}{2\nu} \text{ and } \mathbb{S}=\frac{\nu}{D}.$$

The boundary settings (6) will take the form

$$f(1)=f_w,\ f'(1)=\theta(1)=\phi(1)=1,\ f'(\infty)\to 0,$$

$$\theta(\infty)\to 0,\ \phi(\infty)\to 0 \tag{11}$$

3.0 Results and Discussion

The mathematical calculation has been led for various instances of the Casson factor λ, the Reynolds number $\mathbb{R}$, the Prandtl number $\mathbb{P}$, the heat source/sink parameter Q and Schmidt number $\mathbb{S}$. To understand the physical model carefully, the horizontal velocity, temperature and concentration profiles are deliberated. The mathematical outcomes are represented through graphs in Figure 1–11. The velocity profiles are shown in (Figures 1-3), the temperature outlines in (Figures 4-6) and concentration profiles (Figures 7, 8). The properties of the appropriate factors on the skin friction is shown in Figure 9, the wall temperature gradient in Figure 10 and Sherwood number in Figure 11.

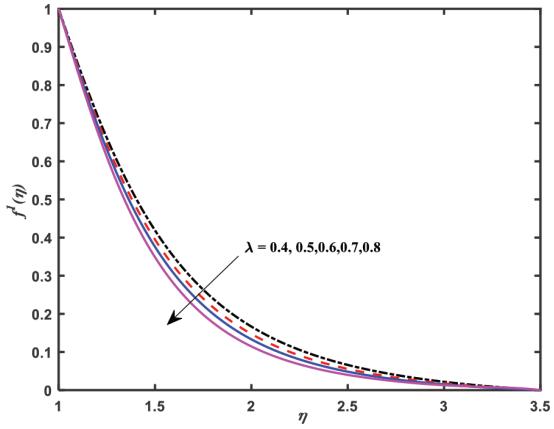


Figure 1. Influence of Casson factor on velocity for $\mathbb{P}=0$, $\mathbb{R}=3$, $Q=1, f_w=-0.1$, $\mathbb{S}=1.5$.

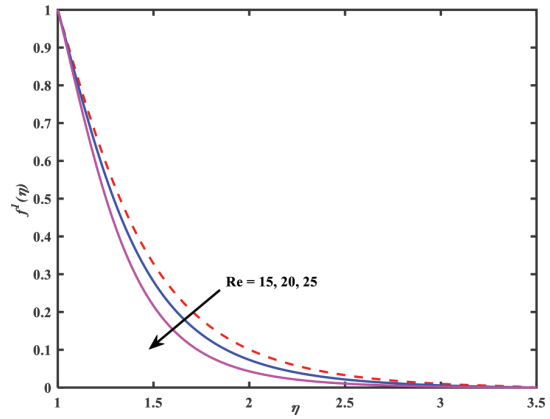


Figure 2. Influence of Reynolds number on velocity for $\mathbb{P}=0$, $\lambda=5$, $Q=1, f_w=-0.1, \mathbb{S}=1.5$.

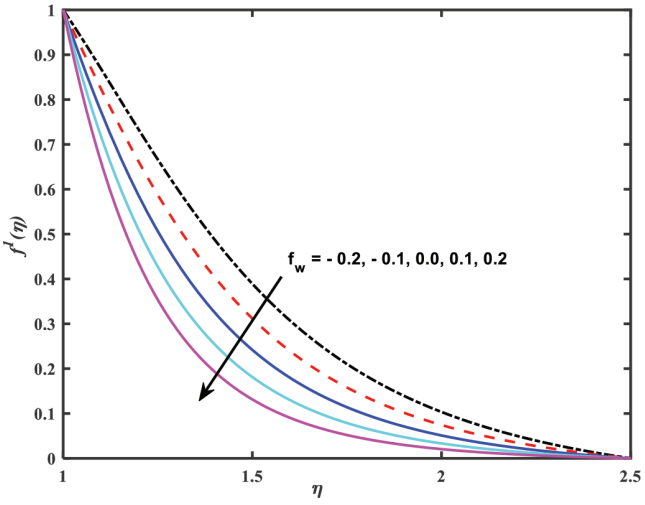


Figure 3. Impact of suction/injection parameter on velocity when Pr=10, Re=25, $Q=1$, Sc=1.5, $\lambda=1$.

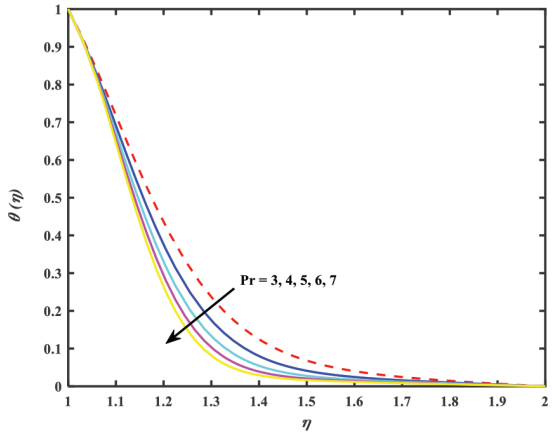


Figure 4. Impact of Prandtl number on temperature profile for $\mathbb{P}=2$, $\mathbb{R}=0$, $Q=1$, $f_w=-0.1$, $\delta=1.5$, $\lambda=1$.

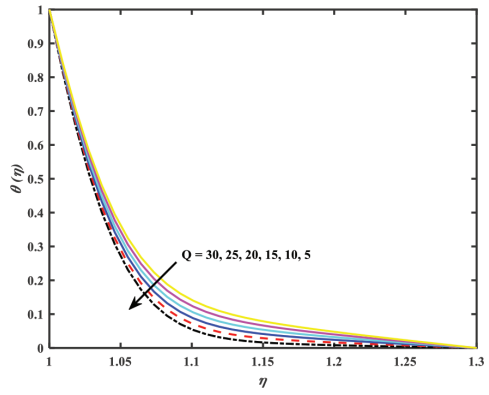


Figure 5. Influence of radiation factor on temperature profile for $\mathbb{P}=2$, $\mathbb{R}=0$, $Q=1$, $f_w=0.0$, $\delta=1.5$, $\lambda=1$.

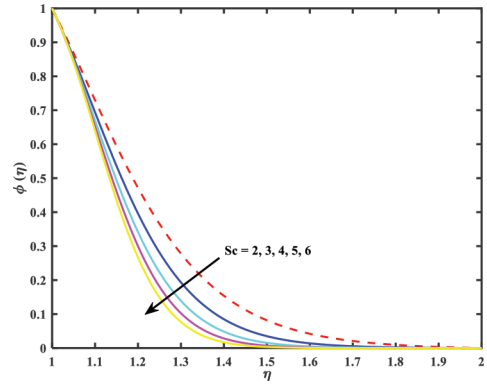


Figure 6. Impact of Schmidt number on concentration profile for $\mathbb{P}=2$, $\mathbb{R}=0$, $Q=1$, $f_w=-0.1$, $\delta=1.5$, $\lambda=1$.

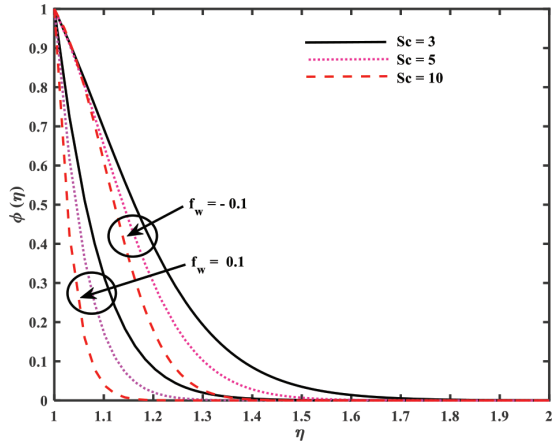


Figure 7. Impact of Schmidt number and suction/injection on concentration profile for $\mathbb{P}=0$, $\mathbb{R}=0$, $Q=1$, $\lambda=1$.

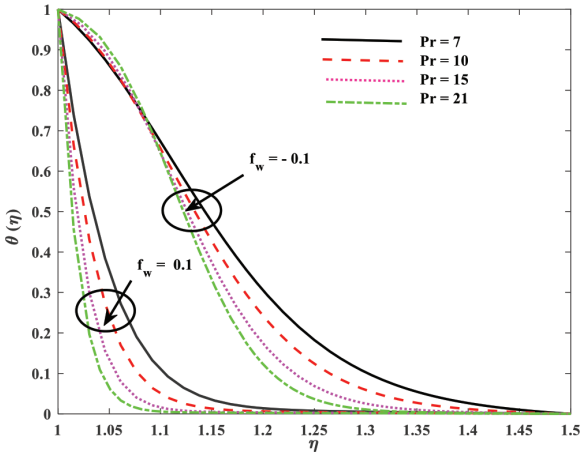


Figure 8. Impact of Prandtl number and suction/injection on temperature profile for $\mathbb{P}=0.7$, $\mathbb{R}=0$, $Q=1$, $\lambda=1$, $\delta=0$.

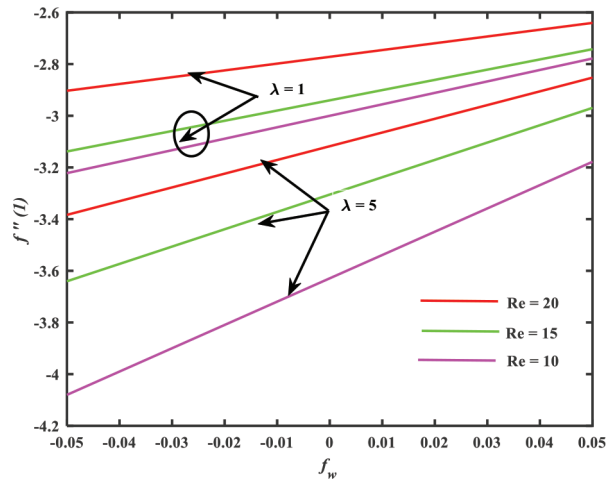


Figure 9. Variation of $f''(0)$ on $\mathbb{R}$ and λ with suction/injection on for $\mathbb{P} = 7$, $\mathbb{R} = 0$, $Q = 1$, $\delta = 0$.

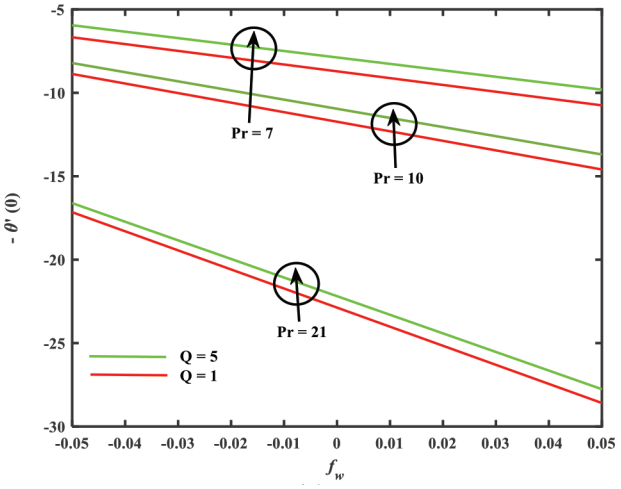


Figure 10. Variation of $-\theta'(0)$ on $\mathbb{P}$ and Q with suction/injection on for $\mathbb{R} = 0$, $\lambda = 1$, $\delta = 0$.

Figure 1 and Figure 2 describe the properties of the Casson factor λ, the Reynolds number Re on horizontal velocity $f'(\eta)$. From Figure 1 we saw that the increasing values of λ reduces velocity and henceforth boundary layer wideness increases near the cylindrical surface. However for greater values of λ the fluid behaves like a Newtonian fluid and further withdraws from plastic flow. The higher values of the Casson factor λ indicates falling yield stress . This serves the fluid to flow easily. The velocity curves in Figure 1 shows that the degree of transport is significantly decreased with the rise of λ.

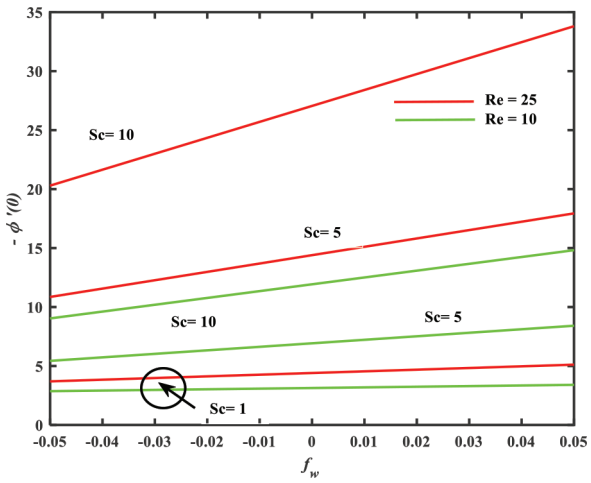


Figure 11. Variation of $-\phi'(0)$ on δ and $\mathbb{R}$ with suction/injection on for $\mathbb{P} = 0.7$, $\lambda = 1$, $Q = 5$.

Figure 2 represents velocity profiles for various values of Reynolds number Re. The velocity decreases with increasing values of Re. Reynolds number characterises the relative importance of the inertia effect to the viscous force. The velocity approaches zero at some large distance from tube surface. The boundary layer thickness falls with rise in Reynolds parameter. This is because of the fact that the inertia effect is more compared to the viscous force, so that the velocity is almost zero from unlimited distance from the tube surface.

Figure 3 depicts the consequence of suction/blowing factor on the velocity of the fluid. It should be observed that when $f_w > 0$, it indicates mass suction and when $f_w < 0$ it indicates mass injection. For increasing values of $f_w > 0$ the velocity falls and $f_w < 0$ for the velocity rises. The rise of f_w results in the diminishing of the boundary layer. So this causes decrease in velocity flow rate.

In Figure 4, the impact of Prandtl number $\mathbb{P}$ on the temperature profiles are detected. It has been witnessed that the temperature drops with growth in the Prandtl number Pr. Furthermore, the thermal boundary layer width also shrinks. It actually means that the flow with great Prandtl number avoids the dispersal of the heat in fluid.

Figure 5 exhibit temperature circulation for several values of heat source/sink factor Q. Here we witness the circulation of temperature near the boundary layer and it is identified that it is poorer at the boundary layer when

there is heat sink whereas the temperature raises for the heat source. Substantially $Q > 0$ infers $T_w > T_\infty$ here we can see supply of heat to the flow area from the wall. Similarly, $Q < 0$ infers $T_w < T_\infty$ in this case there is transfer of heat from flow area to the wall. The impact of growth in the values of the heat source/sink factor Q is to rise the temperature.

In Figure 6 the nature of Schmidt number with respect to the mass fraction field is observed. Since Schmidt number is inversely dependent on the molecular diffusivity, as Schmidt number rises there will be a decline in the concentration field. This reduction in the solutal concentration induces fall in the buoyancy effect of the fluid, causing a reduced induced movement towards the tube surface.

In Figure 7 the influence of concentration profiles for various cases of (δ) for both suction $f_w > 0$ and injection constraint $f_w < 0$ is documented. It is witnessed that for both cases of f_w the concentration drops with rise in Schmidt number (δ). But when $f_w < 0$, i.e for the injection case the thickness of the concentration profiles are almost zero which are far away from the tube surface, whereas for the suction case thickness of the concentration is less. In Figure 8 the same observation is noticed for temperature for increase in values of the Prandtl parameter.

Figure 9 is plotted to observe behaviour of wall shear stress against the suction/injection constraint f_w. The skin friction values linearly increase with rising values of f_w. The velocity gradient declines with rise in Casson factor (λ) and hikes with progress in Reynolds number. Because of the influence of all these factors, there will be a thicker boundary layer and hence there will be an increase in the viscosity of the fluid. whereas Reynolds number lean reverse due to rise in inertial forces inside the fluid. As a consequence, skin friction was amplified in the instance of $\mathbb{R}$.

Figure 10 explains the behaviour of Nusselt number against the suction/injection factor $f_w < 0$. For different parameters Q and $\Pr$, Local Nusselt quantity is inversely found to reduce marginally as Casson fluid factor is amplified. By enhancing λ values, fewer heat is transported from the cylinder surface to the fluid region, subsequently lesser temperatures in the system exterior to the cylinder and lesser local Nusselt numbers, are detected as in Figure 10. This is because of the increasing values of Prandtl number prevents the spreading of the heat in the fluid. So the thermal boundary layer thickness decreases consequently there will be defragmentation of temperature gradient near the wall.

Figure 11 shows the behaviour of Sherwood number against the suction/injection parameter $f_w < 0$. for different parameters $\mathbb{R}$ and δ , $-\phi'(0)$ increases with increase of Schmidt number and Reynolds number this is because of the fact that progress in concentration of the Casson fluid declines the boundary layer wideness of the cylindrical stretching tube.

4.0 Conclusion

- Increasing the values of casson parameter and Reynolds number decreases the velocity boundary layer thickness near the cylindrical surface
- Increasing the values of Prandtl number decreases the thermal boundary layer thickness
- Increase in Reynolds number decreases the velocity boundary layer thickness
- Increase in Schmidt number decreases the concentration boundary layer thickness
- Velocity boundary layer thickness decreases with suction increases with injection.
- Mass transfer increases with increase in Schmidt number and Reynolds number

5.0 References

1. Bachok N, Ishak A, Pop I. Boundary layer stagnation-point flow and heat transfer over an exponentially stretching/shrinking sheet in a nanofluid. Int J Heat Mass Transf. 2012; 55(25-26):8122-8. https://doi.org/10.1016/j.ijheatmasstransfer.2012.08.051
2. Wang CH. Fluid flow due to a stretching cylinder. Phys Fluids. 1988; 31(3):466-6. https://doi.org/10.1063/1.866827
3. Ishak A, Nazar R, Pop I. Uniform suction/blowing effect on flow and heat transfer due to a stretching cylinder. Appl Math Model. 2008; 32(10):2059-66. https://doi.org/10.1016/j.apm.2007.06.036
4. Wang CY, Ng CO. Slip flow due to a stretching cylinder. Int J Non-Linear Mech. 2011; 46(9):1191-4. https://doi.org/10.1016/j.ijnonlinmec.2011.05.014
5. Ashorynejad HR, Sheikholeslami M, Pop I, Ganji DD. Nanofluid flow and heat transfer due to a stretching cylinder

in the presence of magnetic field. Heat Mass Transf. 2013; 49(3):427-36. https://doi.org/10.1007/s00231-012-1087-6
6. Ferdows M, Murtaza MG, Tzirtzilakis EE, Alzahrani F. Numerical study of blood flow and heat transfer through stretching cylinder in the presence of a magnetic dipole. J Appl Math Mech. 2020; 100(7). https://doi.org/10.1002/zamm.201900278
7. Sohail M, Naz R. Modified heat and mass transmission models in the magnetohydrodynamic flow of Sutterby nanofluid in stretching cylinder. Phys A Statis Mech Appl. 2020; 549:124088-8. https://doi.org/10.1016/j.physa.2019.124088
8. Mabood F, Tlili I, Shafiq A. Features of inclined magnetohydrodynamics on a second-grade fluid impinging on vertical stretching cylinder with suction and Newtonian heating. Math Meth Appl Sci. https://doi.org/10.1002/mma.6489
9. Nadeem A, Nadeem S, Saleem A, Malik MY, Issakhov A, Alharbi FM. Models base study of inclined MHD of hybrid nanofluid flow over nonlinear stretching cylinder. Chin J Phys. 2021; 69:109-17. https://doi.org/10.1016/j.cjph.2020.11.019
10. Abbasi A, Mabood F, Farooq W, Hussain Z. Non-orthogonal stagnation point flow of Maxwell nano-material over a stretching cylinder. Int Commun Heat Mass Transf. 2021; 120:105043. https://doi.org/10.1016/j.icheatmasstransfer.2020.105043
11. Kumar RN, Gowda RP, Abusorrah AM, Mahrous YM, Abu-Hamdeh NH, Issakhov A *et al*. Impact of magnetic dipole on ferromagnetic hybrid nanofluid flow over a stretching cylinder. Physica Scripta. 2021; 96(4):045215.
12. Islam S, Khan A, Kumam P, Alrabaiah H, Shah Z, Khan W, *et al*. Radiative mixed convection flow of Maxwell nanofluid over a stretching cylinder with joule heating and heat source/sink effects. Scientific Reports. 2020; 10(1). https://doi.org/10.1038/s41598-020-74393-2
13. Uma M, Dinesh P A. Effects of radiation absorption, soret and dufour on couette flow in an irregular channel for dusty viscoelastic fluid. Int J Sci, Technol, Eng Manag. 2019; 1(4):24-30.
14. Dinesh PA, Vasudevamurthy AS, Uma M. Effects of Forchheimer, MHD and radiation absorption for chemically reacting unsteady dusty viscoelastic fluid couette flow in an irregular channel. Lect. Notes Mech Eng. 2020; 999-1012. https://doi.org/10.1007/978-981-15-4308-1_77
15. Maleki H, Alsarraf J, Moghanizadeh A, Hajabdollahi H, Safaei MR. Heat transfer and nanofluid flow over a porous plate with radiation and slip boundary conditions. J Cent South Univ. 2019; 26(5):1099-115. https://doi.org/10.1007/s11771-019-4074-y
16. Alnaqi AA, Aghakhani S, Pordanjani AH, Bakhtiari R, Asadi A, Tran MD. Effects of magnetic field on the convective heat transfer rate and entropy generation of a nanofluid in an inclined square cavity equipped with a conductor fin: Considering the radiation effect. Int J Heat Mass Transf. 2019; 133:256-67. https://doi.org/10.1016/j.ijheatmasstransfer.2018.12.110
17. Peiravi MM, Alinejad J. Hybrid conduction, convection and radiation heat transfer simulation in a channel with rectangular cylinder. J Therm Anal Calorim. 2019; 140(6):2733-47. https://doi.org/10.1007/s10973-019-09010-0
18. Makinde OD, Ogulu A. The effect of thermal radiation on the heat and mass transfer flow of a variable viscosity fluid past a vertical porous plate permeated by a transverse magnetic field. Chem Eng Commun. 2008; 195(12):1575-84. https://doi.org/10.1080/00986440802115549
19. Sreedevi P, Sudarsana Reddy P. Heat and mass transfer analysis of MWCNT-kerosene nanofluid flow over a wedge with thermal radiation. Heat Transf. 2020; 50(1):10-33. https://doi.org/10.1002/htj.21892
20. Reddy PS, Sreedevi P. Impact of chemical reaction and double stratification on heat and mass transfer characteristics of nanofluid flow over porous stretching sheet with thermal radiation. Int J Ambient Energy. 2020: 1626-36. https://doi.org/10.1080/01430750.2020.1712240
21. Khan MI, Waqas M, Hayat T, Alsaedi A. A comparative study of Casson fluid with homogeneous-heterogeneous reactions. J Colloid Interface Sci. 2017; 498:85-90. https://doi.org/10.1016/j.jcis.2017.03.024
22. Shankar S, Ramakrishna S, Gullapalli N, Samuel N. Triple diffusive MHD casson fluid flow over a vertical wall with convective boundary conditions. Biointerface Res Appl Chem. 2021; 11(6):13765-78. https://doi.org/10.33263/BRIAC116.1376513778
23. Kumar KA, Sugunamma V, Sandeep N. Effect of thermal radiation on MHD Casson fluid flow over an exponentially stretching curved sheet. J Therm Anal Calorim. 2019; 140(5):2377-85. https://doi.org/10.1007/s10973-019-08977-0
24. Hamid M, Usman M, Khan ZH, Ahmad RR, Wang W. Dual solutions and stability analysis of flow and heat transfer of Casson fluid over a stretching sheet. Phys Lett A. 2019; 383(20):2400-8. https://doi.org/10.1016/j.physleta.2019.04.050
25. Raza J. Thermal radiation and slip effects on Magnetohydrodynamic (MHD) stagnation point flow of Casson fluid over a convective stretching sheet. Propuls Power Res. 2019; 8(2):138-46. https://doi.org/10.1016/j.jppr.2019.01.004
26. Das S, Mondal H, Kundu PK, Sibanda P. Spectral quasi-linearization method for Casson fluid with homogeneous heterogeneous reaction in presence of nonlinear thermal radiation over an exponential stretching sheet. Multidiscip Model Mater Struct. 2019; 15(2):398-417.
27. Mahdy A. Heat transfer and flow of a Casson fluid due to a stretching cylinder with the soret and dufour effects. J Eng Phys Thermoph. 2015; 88(4):928-36. https://doi.org/10.1007/s10891-015-1267-6